PROCEEDINGS OF SCIENCE

The onset of jet-ISM interaction in the Seyfert galaxy NGC 3079: VLBI study of OH absorption at sub-pc scale

Dong-Jin Kim,[a,*] **Thomas P. Krichbaum,**[a] **Christian Henkel,**[a,b] **Violette Impellizzeri,**[c] **Francoise Combes,**[d] **Uwe Bach,**[a] **Rainer Mauersberger**[a] **and Anton Zensus**[a]

[a] *Max-Planck-Institut für Radioastronommie*
Auf dem Hügel 69, Bonn, Germany
[b] *Astron. Dept*
King Abdulaziz University, P.O. Box 80203, 21589 Jeddah, Saudi Arabia
[c] *Leiden Observatory—Allegro*
Leiden University, P.O. Box 9513, 2300 RA Leiden, The Netherlands
[d] *Observatoire de Paris*
LERMA, College de France, CNRS, PSL Univ, Sorbonne University, F-75014 Paris, France,
E-mail: dongjin@mpifr.de

NGC 3079 is a Seyfert galaxy, which harbors a compact parsec scale radio jet in its centre. Single dish observations reveal OH absorption lines at 6 cm in front of the continuum radio jet, indicating the presence of ambient molecular gas surrounding the jet. However, its spatial and physical relation to the jet is not yet clear due to the lack of high-resolution observations. To shed light on this matter, we have conducted spectral line VLBI observations using the European VLBI Network (EVN). The OH absorption feature near the systemic velocity of NGC 3079 appears in both, the approaching and the receding jet components, but the blue-shifted (130 km s^{-1}) absorption is only detected on the tip of the approaching radio jet. The observed velocity is not in accord with the sense of rotation of the pc scale H_2O maser disk or sub-kpc scale circumnuclear disk seen in HCN, and thus the blue-shifted absorption is interpreted as a jet-driven outflow. An outward moving jet component seems to accumulate and compress the ambient gas, forming a working surface and absorbing layer, which surrounds the jet head. This scenario is supported by the observed deceleration and brightening of the outer jet component. Follow-up spectral line VLBI studies are desirable to monitor this jet-ISM interaction and to further quantify it.

**** European VLBI Network Mini-Symposium and Users' Meeting (EVN2021) ****
**** 12-14 July, 2021 ****
**** Online ****

*Speaker

© Copyright owned by the author(s) under the terms of the Creative Commons Attribution-NonCommercial-NoDerivatives 4.0 International License (CC BY-NC-ND 4.0).

PoS(EVN2021)038

1. Introduction

NGC 3079 is a nearby Seyfert galaxy (16.0 Mpc, 1 mas=0.08 pc), exhibiting both active galactic nucleus (AGN) activity and active star formation. Kilo-parsec scale radio lobes and super-bubbles show energetic feedback from the radio jet or from star-formation [1–3]. The mass of the central supermassive black hole (SMBH) was estimated to be $(2.39 \pm 0.06) \times 10^6 M_\odot$ [4]. NGC 3079 is classified to be a radio-quiet AGN by its low radio loudness [$R \sim 3$, 5, 6]. The radio loudness R is defined as the flux ratio between the radio (at 5 GHz) and optical (at 4400 Å) bands [7]. Continuum cm-VLBI imaging revealed a parsec scale young radio jet and H_2O maser emission located in a disk [8, 9]. Blue-shifted OH absorption lines hint at the presence of a molecular outflow or represent the receding part of the rotating nuclear disk, but solid evidence is pending due to the lack of high-resolution observations towards the obscuring gas [10, 11]. The radio jet axis is not oriented perpendicular to the pc scale H_2O maser disk or sub-kpc scale circumnuclear disk and is also not aligned with the kpc-scale radio lobes. In the continuum, the individual jet components move at sub-relativistic speeds or are stationary [8] (hereafter M07). 3D hydrodynamic simulations of the interaction of AGN jets with the surrounding interstellar medium (ISM) show that low-power and slow radio jets with inclined geometry with respect to the galactic disk couple more efficiently with the ambient ISM [12, 13]. Previous spectral VLBI observations of the 1.6 GHz OH absorption line demonstrated the feasibility of absorption line imaging, but the angular resolution (FWHM~70 mas) was not sufficient to resolve the OH absorption features on the individual jet components [10]. Here we present a new absorption line imaging VLBI study of NGC 3079, using the excited OH line at 6 GHz, previously detected with the 100-m telescope at Effelsberg. With an angular resolution of 1.6 mas (FWHM), the images reveal a factor of $\sim$ 40 sharper view than the previous OH absorption line study at 1.6 GHz [10].

2. Observation

The VLBI observations towards NGC 3079 were carried out at 6 GHz on October 31, 2019 with the European VLBI Network (EVN), and including e-Merlin. In total, twenty telescopes participated in the observations. Target transitions were the OH lines at 6.030 GHz and 6.035 GHz being observed in absorption against the continuum jet of NGC 3079. Eight intermediate frequencies (IFs) were recorded, each with a bandwidth of 32 MHz, resulting in a total bandwidth of 256 MHz. The e-Merlin stations recorded only two IFs each with a bandwidth of 64 MHz. Most EVN stations observed in right and left hand circular polarization. The data were correlated with the EVN software correlator at JIVE (SFXC) with 512 channels for each IF, which provides a velocity resolution of 3 km s^{-1} for the target transitions. The total observing time was about 8 hrs. The nearby calibrator 0954+556 was observed every 30 min for bandpass calibration. Additional flux density measurements and total power spectra were obtained from single-dish observations at 6 GHz with the 100-m Effelsberg telescope on December 6, 2018. The VLBI data reduction was performed using the Astronomical Image Processing System (AIPS) software. The imaging and self-calibration were done with the Difmap package [14]. First, antenna gains and system temperatures (Tsys) were applied after flagging bad data points. Nominal Tsys values were assumed for the e-Merlin stations due to the lack of Tsys measurements. Then, we followed the standard calibration procedure for

PoS(EVN2021)038

spectral line data, which includes amplitude gain, instrumental delay, ionospheric delay, parallactic angle, band-pass shape, multi-band delay (i.e., fringe-fitting), and Doppler shift calibrations. For continuum imaging, the calibrated data were averaged over an integration time of 20 s and over frequency channels, flagging sharp band-edges of about 1 MHz for each IF. The frequency averaged data were further processed in Difmap for phase and amplitude self-calibration and imaging using the CLEAN method. For the 6 GHz OH absorption line imaging, several channels were averaged to increase the imaging sensitivity by using the AIPS task UVLSF, which resulted in a slightly degraded (but still acceptable) spectral resolution of 13 km s^{-1}. The established continuum model from Difmap was applied for the self-calibration of the spectral line data, and the clean process was iterated in each channel to detect the absorption features on the continuum images.

3. Result & Discussion

Fig 1 (left) shows the 6 GHz continuum image of NGC 3079, which reveals four distinct structural components A, B, C, and D (D is termed as E in M07). These components are known and were previously seen in the 5 GHz and 15 GHz images shown by M07. The peak intensity of the new map is 46 mJy beam^{-1}, and the rms noise level is 0.05 mJy beam^{-1}. The high brightness temperatures of the continuum components ($> 4 \times 10^7 K$) indicate synchrotron emission from the AGN jet. The recovered VLBI flux density in the EVN observations was 145.2 mJy. The continuum components are aligned at a position angle 126.2° (A-C-B) and 87.3° (B-D). These position angles are consistent with previous measurements reported in M07. The component A is partially resolved and appears elongated; between A and C also a small gap of emission is seen. The B component is known to be stationary from the phase referencing VLBI observations of M07.

3.1 6 GHz continuum jet and OH absorption lines

The B component was used as the reference position to measure the angular distance between the others. The angular distances between A-B (29.7 mas) and B-D (25.3 mas) were measured by Gaussian fittings on the intensity profiles along the position angles, connecting two continuum components (see Fig. 1). Fig 2 shows the angular distance variation between the A-B and B-D components measured at 5 GHz (2000-2006) from the literature and at 6 GHz for this study [8, 9, 15–17]. The increments of the angular distance are +1.83±0.3 mas (A-B) and -0.49±0.3 mas (B-D) over 15 years. The B and D components seem to be stationary. The angular separation rate of the A component with respect to the B component between 1999-2002 is 0.129±0.03 mas yr^{-1}, which is translated into an apparent speed of 0.034 c. The apparent speed of the A component between 2004-2019 has decreased by a factor of ~2.5 compared to the previous measurement (0.32±0.03 mas yr^{-1}, $v_{app} = 0.084$ c) between 1999-2002 [8]. Interestingly, the flux density of the A component has roughly doubled, whereas the flux densities of the B and D components remained almost constant.

In the EVN observations we detected the 6.030 GHz and 6.035 GHz OH absorption lines. The systemic velocity of NGC 3079 has been estimated from H I (1116 km s^{-1}), the H_2O maser (1125 km s^{-1}), and the CO and HCN disks (1147 km s^{-1}) [9, 11, 18, 19]. In the following we adopt 1147 km s^{-1} as the systemic velocity of NGC 3079 because the sub-kpc scale HCN disk provides a better constraint on the systemic velocity of a compact AGN compared to the extended

PoS(EVN2021)038

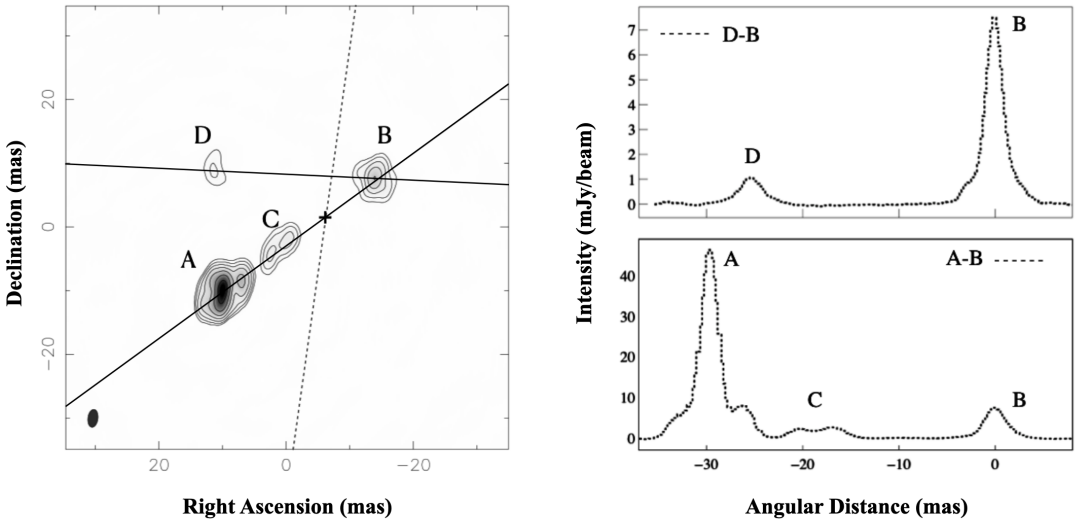

Figure 1: Left: The self-calibrated continuum map of NGC 3079 at 6.0 GHz. Four separated continuum components are labeled with A, B, C, and D. The peak flux density is 46 mJy/beam, and the lowest contour is at 1% of the peak flux with subsequent contours increasing by a factor of 2. The dashed line indicates the location of the H_2O maser disk (PA = 82°), and the solid lines show the alignment between A-B and B-D components. The dynamical center of the H_2O maser disk is marked with a cross [9]. Slices along the B-D and A-B components are shown in the right panel. Right: The intensity profile along the lines connecting the peak position of the component D-B and A-B.

kpc scale H I disk. From this we obtain Doppler velocities of the two OH absorption features at -29 km s^{-1} (hereafter C1) and -130 km s^{-1} (hereafter C2), respectively. The absorption features are shown in Fig.3. The small beam size of the EVN observations resulted in higher absorption depths of the 6 GHz OH absorption lines (blue), when compared with the spectra from our single-dish observations (red). The C2 component shows broader line widths and deeper absorption depths than C1. Fig 4 shows the spatial distribution of the two OH absorption features. C2 (V_{peak}:-130 km s^{-1}) is located at the A component, and C1 (V_{peak}:-29 km s^{-1}) was detected at the A and B components. If the absorbing gas is a part of the circumnuclear disk, red-shifted absorption would be expected at the A component [19], but we detected a blue-shifted absorption feature. Therefore, the most plausible explanation of the 6 GHz OH absorption on the A component is a molecular outflow which is related to or even driven by the expanding radio jet.

3.2 Jet-ISM interaction in NGC 3079

The radio jet and their ambient OH cloud(s) which are revealed by these EVN observations likely mark jet-ISM interaction in the Seyfert galaxy NGC 3079. We find that the jet component A is decelerating and its flux density is increasing. Jet-ISM interaction can cause jet deceleration via momentum transfer from jet to the interacting medium. The jet-ISM interaction compresses the ambient medium and increases the external pressure on the jet, which could lead to the observed flux density increase [8]. The broader line width and higher column density of the blue-shifted OH absorption (C2) with respect to the non-outflow absorption (C1) manifests an increased local

PoS(EVN2021)038

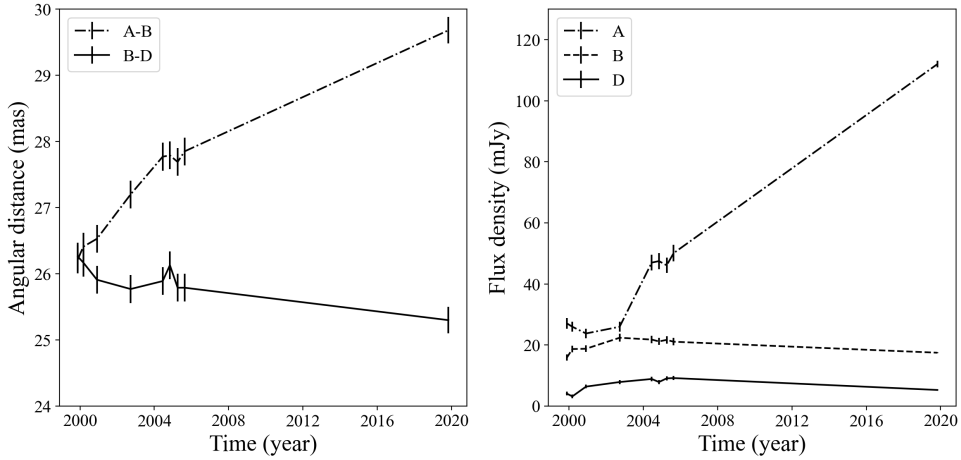

Figure 2: Left: The angular separation between the continuum components A-B and B-D plotted versus time for the past 20 years. Flux density and location of the individual jet components were taken from M07. The lines connecting the data points show the proper motion. Right: Variation of the flux density for the three jet components.

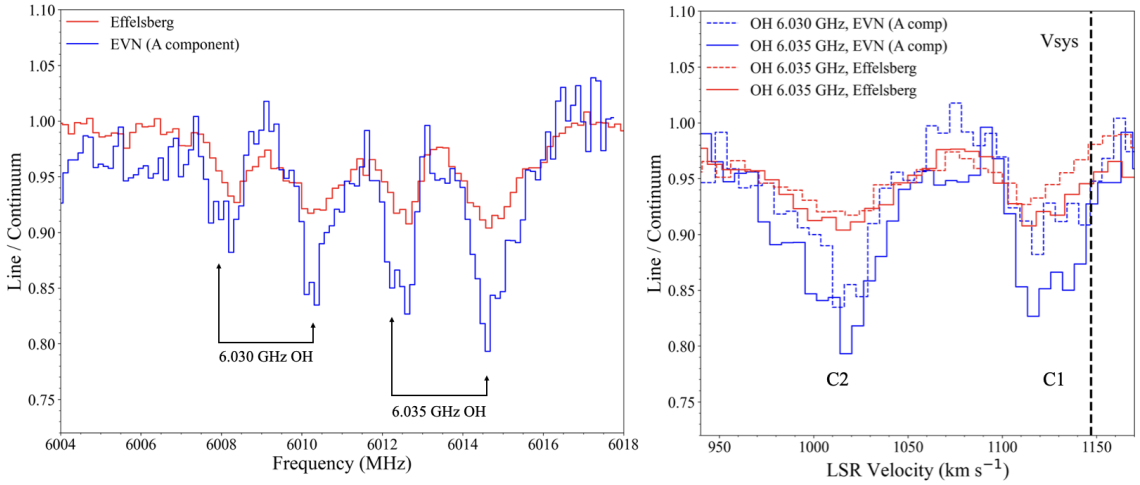

Figure 3: Left: Comparison of the 6 GHz OH absorption lines from the Effelsberg (red) and the EVN observations (blue) in Dec 2018, and Oct 2019, respectively. The EVN spectrum was observed towards the A component. Right: 6.030 GHz and 6.035 GHz OH absorption lines aligned on the velocity axis. The systemic velocity of NGC 3079 (1147 km s^{-1}) is marked by the dotted vertical line.

column density and velocity dispersion of the jet-driven outflows. Blue-shifted SiO and H^{13}CN absorption lines detected at 3 mm from NOEMA observations show blue-shifted feature up to 350 km s^{-1}, further supporting the presence of molecular outflows [11].

The dynamical mass of the circumnuclear HCN disk was estimated to be $\sim 10^{9.3} M_{\odot}$ [11]. The escape velocity at the measured radius of the HCN disk (at 112 pc) is 391 km s^{-1}. If the jet component A is located within a few pc from the jet launching region and no further kinetic energy is transferred from the jet, the jet-driven OH outflow (130 km s^{-1}) will not propagate over the circumnuclear disk. A bright ionized emission, which is well aligned with the radio jet axis

PoS(EVN2021)038

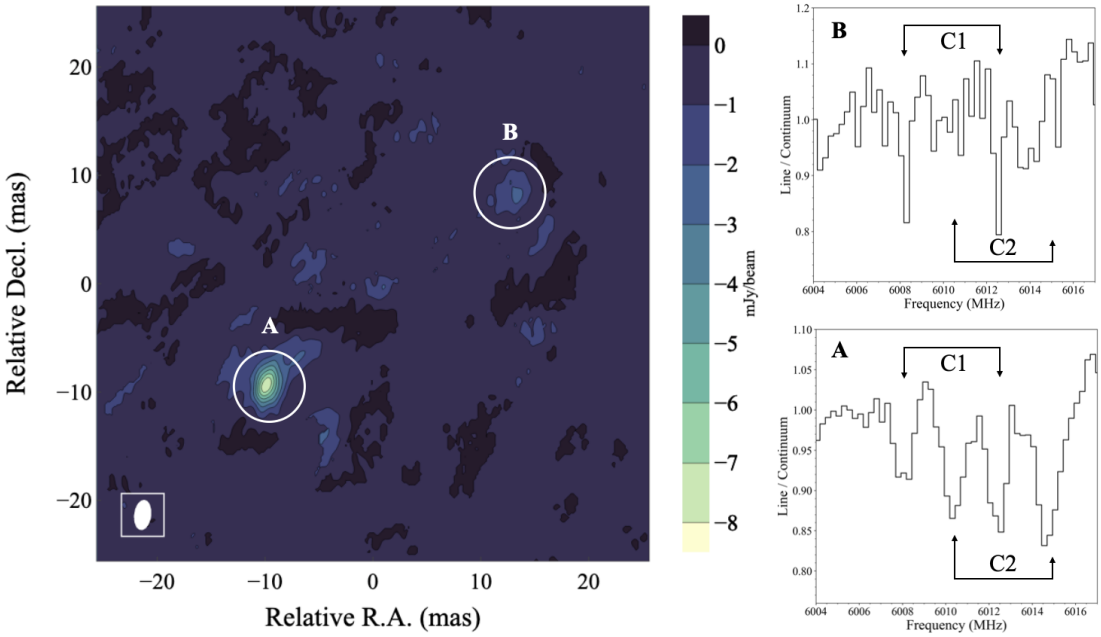

Figure 4: Spatial distribution of the 6 GHz OH absorption lines. **Right**: Averaged OH absorption spectra towards the A and B continuum components. The C1 (V_{peak}:-29 km s^{-1}) and C2 (V_{peak}:-130 km s^{-1}) features are detected towards A, but towards B only the C1 feature is seen.

about 250 pc from the jet-launching region [2], is attributed to the results of previous episodic radio jet activities. We note that the jet-driven molecular outflow occurs at a distance of a few pc from the central engine, disrupting the ambient medium. Therefore, the molecular outflow might facilitate AGN fueling by removing angular momentum of the rotating circumnuclear disk or clumpy molecular clouds. In this process, the relative geometry of radio jet and circumnuclear disk is an important factor, determining the significance of jet-ISM interaction [20].

4. Conclusions

We carried out a high-resolution VLBI study on the circumnuclear gas of the Seyfert galaxy NGC 3079. 6 GHz OH absorption observations using the EVN reveal a strong interaction between propagating jet and its ambient medium on the sub-pc scale. The main findings are summarized as follows:

1. Two separated absorption features were detected in both the 6.030 and 6.035 GHz OH lines. Absorption around the systemic velocity of NGC 3079 (C1 = OH_{sys}) appears in both approaching and receding jets, but the blue-shifted (C2 = OH_{blue}) absorption is only present in the approaching jet. The OH_{blue} is interpreted as a jet-driven outflow, considering the rotation direction of the circumnuclear disk of NGC 3079.

2. Higher OH absorption depths and broader line widths are measured in the C2 feature rather than in C1. This may indicate an enhanced local density and turbulence of nuclear gas caused by jet-ISM interactions at the working surface of the outward propagating jet. The

PoS(EVN2021)038

molecular outflow might be confined at sub-pc scales, but it would increase the accretion rate by removing angular momentum from the circumnuclear disk in NGC 3079.

3. The impact of the jet-ISM interaction on the radio jet properties is also seen in the continuum VLBI data. The propagating jet component A shows significant deceleration, and a brightening flux density at the south-eastern end of the jet. These findings support a frustrated jet scenario, in which a low power radio jet works against the ambient medium of a Seyfert galaxy.

References

[1] S. Veilleux, G. Cecil, J. Bland-Hawthorn, R.B. Tully, A.V. Filippenko and W.L.W. Sargent, *The Nuclear Superbubble of NGC 3079*, **433** (1994) 48.

[2] G. Cecil, J. Bland-Hawthorn, S. Veilleux and A.V. Filippenko, *Jet- and Wind-driven Ionized Outflows in the Superbubble and Star-forming Disk of NGC 3079*, **555** (2001) 338 [astro-ph/0101010].

[3] B. Sebastian, P. Kharb, C.P. O'Dea, E.J.M. Colbert and S.A. Baum, *The Filamentary Radio Lobes of the Seyfert-Starburst Composite Galaxy NGC 3079*, **883** (2019) 189 [1907.12765].

[4] B.L. Davis, A.W. Graham and M.S. Seigar, *Updating the (supermassive black hole mass)-(spiral arm pitch angle) relation: a strong correlation for galaxies with pseudobulges*, **471** (2017) 2187 [1707.04001].

[5] V.A. Taylor, R.A. Jansen, R.A. Windhorst, S.C. Odewahn and J.E. Hibbard, *UBVR and Hubble Space Telescope Mid-Ultraviolet and Near-Infrared Surface Photometry and Radial Color Gradients of Late-Type, Irregular, and Peculiar Galaxies*, **630** (2005) 784 [astro-ph/0506122].

[6] C.M.V. Impellizzeri, C. Henkel, A.L. Roy and K.M. Menten, *6.7 GHz methanol absorption toward the Seyfert 2 galaxy NGC 3079*, **484** (2008) L43 [0805.1063].

[7] K.I. Kellermann, R.A. Sramek, M. Schmidt, R.F. Green and D.B. Shaffer, *The Radio Structure of Radio Loud and Quiet Quasars in the Palomar Bright Quasar Survey*, **108** (1994) 1163.

[8] E. Middelberg, I. Agudo, A.L. Roy and T.P. Krichbaum, *Jet-cloud collisions in the jet of the Seyfert galaxy NGC3079*, **377** (2007) 731 [astro-ph/0702481].

[9] P.T. Kondratko, L.J. Greenhill and J.M. Moran, *Evidence for a Geometrically Thick Self-Gravitating Accretion Disk in NGC 3079*, **618** (2005) 618 [astro-ph/0408549].

[10] Y. Hagiwara, H.-R. Klöckner and W. Baan, *VLBI imaging of OH absorption: the puzzle of the nuclear region of NGC3079*, **353** (2004) 1055 [astro-ph/0404347].

PoS(EVN2021)038

[11] M.-Y. Lin, R.I. Davies, L. Burtscher, A. Contursi, R. Genzel, E. González-Alfonso et al., *Thick discs, and an outflow, of dense gas in the nuclei of nearby Seyfert galaxies*, **458** (2016) 1375 [1602.06452].

[12] D. Mukherjee, G.V. Bicknell, R. Sutherland and A. Wagner, *Relativistic jet feedback in high-redshift galaxies - I. Dynamics*, **461** (2016) 967 [1606.01143].

[13] D. Mukherjee, A.Y. Wagner, G.V. Bicknell, R. Morganti, T. Oosterloo, N. Nesvadba et al., *The jet-ISM interactions in IC 5063*, **476** (2018) 80 [1801.06875].

[14] M.C. Shepherd, *Difmap: an Interactive Program for Synthesis Imaging*, in *Astronomical Data Analysis Software and Systems VI*, G. Hunt and H. Payne, eds., vol. 125 of *Astronomical Society of the Pacific Conference Series*, p. 77, Jan., 1997.

[15] J.A. Irwin and E.R. Seaquist, *Nuclear Jets in the Radio Lobe Spiral Galaxy NGC 3079*, **335** (1988) 658.

[16] A.S. Trotter, L.J. Greenhill, J.M. Moran, M.J. Reid, J.A. Irwin and K.-Y. Lo, *Water Maser Emission and the Parsec-Scale Jet in NGC 3079*, **495** (1998) 740 [astro-ph/9712086].

[17] S. Sawada-Satoh, M. Inoue, K.M. Shibata, S. Kameno, V. Migenes, N. Nakai et al., *The Nuclear Region of the Seyfert 2 Galaxy NGC 3079*, **52** (2000) 421.

[18] N. Shafi, T.A. Oosterloo, R. Morganti, S. Colafrancesco and R. Booth, *The 'shook up' galaxy NGC 3079: the complex interplay between H I, activity and environment*, **454** (2015) 1404 [1509.00350].

[19] J. Koda, Y. Sofue, K. Kohno, H. Nakanishi, S. Onodera, S.K. Okumura et al., *Nobeyama Millimeter Array CO (J=1-0) Observations of the Hα/Radio Lobe Galaxy NGC 3079: Gas Dynamics in a Weak Bar Potential and Central Massive Core*, **573** (2002) 105 [astro-ph/0210613].

[20] D. Mukherjee, G.V. Bicknell, A.Y. Wagner, R.S. Sutherland and J. Silk, *Relativistic jet feedback - III. Feedback on gas discs*, **479** (2018) 5544 [1803.08305].

PoS(EVN2021)038